

Motion of Chern-Simons number at High Temperatures under a Chemical Potential

Guy D. Moore¹

Princeton University

*Joseph Henry Laboratories, PO Box 708
Princeton, NJ 08544, USA*

Abstract

I investigate the evolution of finite temperature, classical Yang-Mills field equations under the influence of a chemical potential for Chern Simons number N_{CS} . The rate of N_{CS} diffusion, Γ_d , and the linear response of N_{CS} to a chemical potential, Γ_μ , are both computed; the relation $\Gamma_d = 2\Gamma_\mu$ is satisfied numerically and the results agree with the recent measurement of Γ_d by Ambjorn and Krasnitz. The response of N_{CS} under chemical potential remains linear at least to $\mu = 6T$, which is impossible if there is a free energy barrier to the motion of N_{CS} . The possibility that the result depends on lattice artefacts via hard thermal loops is investigated by changing the lattice action and by examining elongated rectangular lattices; provided that the lattice is fine enough, the result is weakly if at all dependent on the specifics of the cutoff. I also compare $SU(2)$ with $SU(3)$ and find $\Gamma_{SU(3)} \sim 7(\alpha_s/\alpha_w)^4 \Gamma_{SU(2)}$.

1 Introduction

Baryon number is violated in the Standard Model[1]. While it is conserved to all orders in perturbation theory, nonperturbative effects involving topologically nontrivial gauge and Higgs field configurations permit its violation at a rate which, at zero temperature, is suppressed by an exponent of order $\exp(-4\pi/\alpha_W)$. While this rate is far too low to have any phenomenologically interesting consequences, it should be much larger at high temperatures, perhaps high enough to explain the matter abundance in the universe.

I will briefly review baryon number violation in the Standard Model. Because of the axial anomaly, the Baryon number current is not conserved, but satisfies

$$\partial_\mu J_B^\mu = \frac{-g^2 N_F}{64\pi^2} \epsilon^{\mu\nu\alpha\beta} F_{\mu\nu}^a F_{\alpha\beta}^a, \quad (1)$$

where N_F is the number of generations of fermions and F is the $SU(2)$ field strength tensor. I have left out the hypercharge fields, which are irrelevant because they do not have nontrivial topological properties. For smooth field configurations the righthand side of this equation is a total divergence,

$$\begin{aligned} \frac{g^2}{64\pi^2} \epsilon^{\mu\nu\alpha\beta} F_{\mu\nu}^a F_{\alpha\beta}^a &= \partial^\mu K_\mu \\ K^\mu &= \frac{g^2}{32\pi^2} \epsilon^{\mu\nu\alpha\beta} (F_{\nu\alpha}^a A_\beta^a - \frac{g}{3} \epsilon_{abc} A_\nu^a A_\alpha^b A_{beta}^c). \end{aligned} \quad (2)$$

¹e-mail: guymoore@puhep1.princeton.edu

The charge associated with this quantity, $\int d^3x(K_0)$, is called the Chern-Simons number, N_{CS} . It possesses the important property that, if the field configuration is pure gauge at two times $t = t_0$ and $t = t_1$, then

$$N_{CS}(t_1) - N_{CS}(t_0) = \int_{t_0}^{t_1} dt \int d^3x \frac{g^2}{64\pi^2} \epsilon^{\mu\nu\alpha\beta} F_{\mu\nu}^a F_{\alpha\beta}^a \quad (3)$$

is an integer (assuming only that the gauge field is everywhere smooth). N_{CS} is invariant under small gauge transformations (those which can be built up infinitesimally) and changes by an integer under large gauge transformations; the difference between N_{CS} at two times is gauge invariant, because the righthand side of the last equation is.

The action of a Euclidean process which changes N_{CS} is at least $\int (1/4) F_{\mu\nu}^a F_a^{\mu\nu} \geq 8\pi^2/g^2$, and is in fact even larger, as the nontrivial gauge fields make the Higgs field gradient nonzero as well. If the configuration is of greater spatial extent than the inverse W mass then the Higgs field gradients dominate the action, which will be $\gg 8\pi^2/g^2$. For configurations of very small spatial extent, the asymptotic freedom of the weak coupling g again makes the action grow. Therefore, unlike QCD, topology changes in the electroweak theory are exponentially suppressed, as mentioned above.

However, at finite temperature it is no longer relevant how large the action of a configuration is; the system is excited and there is energy available to make topological transitions. In the broken electroweak phase there is a free energy barrier to such transitions [2, 3], which proceed at an exponentially suppressed rate determined by the temperature and Higgs mass. At higher temperatures electroweak symmetry is restored, so the Higgs gradients no longer inhibit topology changing transitions. For sufficiently large configurations, with spatial extent $O(1/g^2 T)$, the free energy barrier, if any, is parametrically order unity, and baryon number may be violated readily [4]. This is relevant because any $B + L$ (Baryon plus Lepton number) present in the early universe would then be erased, and, during the electroweak phase transition, any $B + L$ separation by the wall of a broken phase bubble would produce a baryon number asymmetry, because the excess on the symmetric phase side would be destroyed, while that on the broken phase side would be preserved[5, 6].

The rate which is relevant to this baryogenesis scenario is probably the rate at which a chemical potential for baryon number, caused by the separation of baryon number across the wall, induces baryon number changing transitions². That is, we need to know

$$\Gamma_\mu = \frac{T \langle -\partial N_{CS}/\partial t \rangle_\mu}{V\mu} \quad (\mu \ll T), \quad (4)$$

where by $\langle \rangle_\mu$ I mean the expectation value when there is a chemical potential μ for N_{CS} (equal to N_F times the chemical potential for baryon number, by Eq. (1)), and V is the volume over which the chemical potential exists.

A detailed balance argument shows that this rate is half the rate for N_{CS} diffusion,

$$\Gamma_d = \lim_{t \rightarrow \infty} \frac{\langle (N_{CS}(t) - N_{CS}(0))^2 \rangle}{Vt} \quad (5)$$

²only probably, because in the realistic problem the chemical potential may only extend over a region of space or time small enough that the large volume or large time limit are not attained

in the absence of a chemical potential. The argument is quite simple in the broken phase; the general case is reviewed in section 2. The nice thing about Γ_d is that it is straightforward to measure it for the classical bosonic theory at finite temperature by lattice techniques, and there is reason to believe that the behavior of this classical system corresponds well to the infrared dynamics of the actual finite temperature, quantum Yang-Mills Higgs system[7].

Based on these ideas, and following previous work[8], Ambjorn and Krasnitz have recently performed extensive numerical simulations of the lattice Yang-Mills system [9] and have demonstrated convincingly that there is a lattice spacing independent classical value for Γ_d . On parametric grounds, $\Gamma_d = \kappa_d(\alpha_w T)^4$; they find $\kappa_d = 1.09 \pm 0.04$. This work apparently answers the question relevant to baryogenesis, but it leaves some open questions. For instance, because the theory has linear divergences, the lattice spacing independence does not necessarily assure the absence of lattice artefacts. Also, the reason why the rate is this value is not at all clear; for instance, in terms of the length scale necessary to eliminate finite lattice volume effects, the rate seems quite small, order 1/100 [11], and it is not clear whether this is the result of a (parametrically order unity) free energy barrier to winding number change, as proposed for instance in [12].

An alternative technique, which can be used to shed some light on these matters as well as to check the result of Ambjorn and Krasnitz, is to apply a chemical potential for N_{CS} on the lattice and look at the rate at which N_{CS} drifts. The method encounters some fairly serious technical difficulties [8], which I will discuss at some length in section 3; I present a possible resolution, which the numerical results of section 4 demonstrate to be successful. I will also show that there is in fact no free energy barrier to topology change in Yang-Mills theory at finite temperature. Section 5 will be devoted to investigations of possible ultraviolet lattice artefacts in the classical lattice simulations. In section 6 I extend the technique to find the strong N_{CS} diffusion rate (I replace the group $SU(2)$ with $SU(3)$). In section 7 I conclude. I present a simple, efficient thermalization algorithm which works for both the $SU(2)$ and $SU(3)$ cases in Appendix A.

2 The Two Rates

As mentioned above, there is a general relation between the N_{CS} diffusion rate Γ_d and the linear response rate to a chemical potential, Γ_μ . This arises from a detailed balance argument as follows.

Let us assume that the generalized coordinate N_{CS} is in thermal contact with a large thermal reservoir, which evolves ergodically, so that over very long time intervals t , correlators involving \dot{N}_{CS} , such as $\langle \dot{N}_{CS}(t)(N_{CS}(t) - N_{CS}(0)) \rangle$, vanish in the absence of a chemical potential, where $\langle \dot{N}_{CS} \rangle = 0$. This is just the condition that the motion of N_{CS} become thoroughly thermalized over long periods of time and it should be satisfied in the realistic case. It is also a necessary condition for a diffusion rate to be well defined. In this case, the probability for a system to go from $N_{CS}(0)$ at time 0 to $N_{CS}(t)$ at time t depends only on those values and t , and the probability that the Chern-Simons number is $N_{CS}(t)$ at time t is, in terms of the probability distribution $\mathcal{P}(N_{CS}(0), 0)$ for its value at time 0,

$$\mathcal{P}(N_{CS}(t), t) = \int dN_{CS}(0) \mathcal{P}(N_{CS}(0), 0) G_t(N_{CS}(0), N_{CS}(t)), \quad (6)$$

where $G_t(N_{CS}(0), N_{CS}(t))$ is the probability that the system, initially at $N_{CS}(0)$, will arrive at time t at $N_{CS}(t)$. G_t is invariant to a simultaneous shift of both arguments by an integer, and in the absence of a chemical potential, it is invariant on exchange of its arguments (by time reversal invariance), and, when one argument is 0, is invariant under a sign change in the other (by parity invariance).

To determine the rate of response to a chemical potential, I want to consider the equilibrium probability distribution when a term μN_{CS} is added to the Hamiltonian. Unfortunately the energy is then unbounded from below and no equilibrium probability distribution exists. I will therefore add a term ϵN_{CS}^2 to the Hamiltonian so that the theory will be well defined; in fact, in the real theory in finite volume there is such a term, because, as N_{CS} changes, the number of fermions slowly builds up and changes the chemical potential. I take ϵ to be much less than any other quantity in the problem and consider the equilibrium probability distribution $\mathcal{P}_\mu(N_{CS})$. The chemical potential changes the Boltzmann factors for different states, so in relation to the distribution without chemical potential,

$$\begin{aligned} \frac{\mathcal{P}_\mu(N_{CS1})}{\mathcal{P}_\mu(N_{CS2})} &= \frac{\mathcal{P}_0(N_{CS1})}{\mathcal{P}_0(N_{CS2})} f_{\text{periodic}}(N_{CS1}, N_{CS2}) \times \exp \frac{-\mu}{T} (N_{CS1} - N_{CS2}) \\ &\simeq \frac{\mathcal{P}_0(N_{CS1})}{\mathcal{P}_0(N_{CS2})} \left(1 - \frac{\mu(N_{CS1} - N_{CS2})}{T} + \frac{\mu^2(N_{CS1} - N_{CS2})^2}{2T^2} \right) \times \\ &\quad \left(1 + \frac{\mu^2}{T^2} f_{\text{periodic}}^1(N_{CS1}, N_{CS2}) \right), \end{aligned} \quad (7)$$

where the function f_{periodic} is periodic on integer changes of either argument and equals 1 when the arguments coincide. Its expansion only contains terms even in μ .

Also, the hopping probability G_t takes on μ dependent corrections

$$G_{t,\mu} = G_t^0 + \frac{\mu}{T} G_t^1 + \frac{\mu^2}{T^2} G_t^2 \quad (8)$$

where G_t^1 satisfies

$$G_t^1(0, N_{CS}(t)) = -G_t^1(0, -N_{CS}(t)) \quad (9)$$

because the chemical potential is odd in N_{CS} . There is also an order ϵ correction which will not be important here.

Using the condition that, for the equilibrium distribution (with or without μ), $\mathcal{P}(N_{CS})$ is time independent, I find

$$\begin{aligned} \mathcal{P}_\mu(0, 0) &= \mathcal{P}_\mu(0, t) = \int dN_{CS}(0) \mathcal{P}_\mu(N_{CS}(0), 0) G_{t,\mu}(N_{CS}(0), 0), \\ \mathcal{P}_0(0, 0) &= \mathcal{P}_0(0, t) = \int dN_{CS}(0) \mathcal{P}_0(N_{CS}(0), 0) G_t^0(N_{CS}(0), 0). \end{aligned} \quad (10)$$

Dividing through by $\mathcal{P}(0, 0)$, I get the equality

$$\int dN_{CS}(0) \frac{\mathcal{P}_\mu(N_{CS}(0), 0)}{\mathcal{P}_\mu(0, 0)} G_{t,\mu}(N_{CS}(0), 0) = \int dN_{CS}(0) \frac{\mathcal{P}_0(N_{CS}(0), 0)}{\mathcal{P}_0(0, 0)} G_t^0(N_{CS}(0), 0), \quad (11)$$

which I can expand in powers of μ , using Eqs. (7) and (8).

At order μ ,

$$\int dN_{CS} \frac{\mathcal{P}_0(N_{CS}, 0)}{\mathcal{P}_0(0, 0)} N_{CS} G_t^0(N_{CS}, 0) = \int dN_{CS} \frac{\mathcal{P}_0(N_{CS}, 0)}{\mathcal{P}_0(0, 0)} G_t^1(N_{CS}, 0), \quad (12)$$

which follows automatically because both sides are zero; the first because, in the theory without chemical potential, $\langle \dot{N}_{CS} \rangle = 0$, and the second because G_t^1 is asymmetric.

At the next order,

$$\int dN_{CS} \frac{\mathcal{P}_0(N_{CS}, 0)}{\mathcal{P}_0(0, 0)} \frac{N_{CS}^2}{2} G_t^0(N_{CS}, 0) = \int dN_{CS} \frac{\mathcal{P}_0(N_{CS}, 0)}{\mathcal{P}_0(0, 0)} N_{CS} G_t^1(N_{CS}, 0) \quad (13)$$

$$- \int dN_{CS} f_{\text{periodic}}^1 \frac{\mathcal{P}_0(N_{CS}, 0)}{\mathcal{P}_0(0, 0)} G_t^0(N_{CS}, 0) \quad (14)$$

$$- \int dN_{CS} \frac{\mathcal{P}_0(N_{CS}, 0)}{\mathcal{P}_0(0, 0)} G_t^2(N_{CS}, 0). \quad (15)$$

The term on the lefthand side is half the mean squared change in N_{CS} between time 0 and time t , in the system without chemical potential; that is, it is $Vt\Gamma_d/2$. The righthand side in the top line is $-T/\mu$ times the mean motion of N_{CS} in time t , with a chemical potential but under the $\mu = 0$ probability distribution; that is, it is $Vt\Gamma_\mu$. The first line is the desired relation, $\Gamma_d/2 = \Gamma_\mu$. All that must be shown is that the remaining terms do not grow linearly with large t .

For (14) this holds because $f_{\text{periodic}}^1 \mathcal{P}_0(N_{CS}, 0)/\mathcal{P}_0(0, 0)$ is bounded, and $\int dN_{CS} G_t^0(N_{CS}, 0)$ is 1 because it is the probability that if the system starts at $N_{CS} = 0$, it will end with any value of N_{CS} . Hence the term as a whole is bounded, independent of t , and cannot grow linearly in the large t limit.

For the second term, (15), we can see that it is bounded at large time by considering the evolution of the system with chemical potential, but when the initial probability distribution is \mathcal{P}_0 , the equilibrium distribution for zero chemical potential. Since the distribution starts out periodic, it must remain periodic, and

$$\mathcal{P}(0, t)/\mathcal{P}(0, 0) = \int dN_{CS} \frac{\mathcal{P}_0(N_{CS}, 0)}{\mathcal{P}_0(0, 0)} \left(G_t^0(N_{CS}, 0) + \frac{\mu}{T} G_t^1(N_{CS}, 0) + \frac{\mu^2}{T^2} G_t^2(N_{CS}, 0) \right) \quad (16)$$

must remain bounded. The G_t^1 term drops because the initial distribution is symmetric, and the G_t^0 term gives 1; the G_t^2 term is the one we want to know, and we see that it is bounded. In fact, I expect that the probability distribution will approach $\mathcal{P}_0(N_{CS}) * f_{\text{periodic}}$ at large t , so the two extra terms (14) and (15) probably cancel; but it is sufficient to show that they remain bounded at large t , which I have now done. Hence the relation $\Gamma_d = 2\Gamma_\mu$ follows. (For an alternative, formal derivation see [13].)

Note that it is essential in the above argument that the typical distance that N_{CS} moves, over a time long compared to the thermalization time, is much less than T/μ , a condition on the size of μ . If there is a free energy barrier between integer values of N_{CS} , then the important typical distance which N_{CS} moves will be at least 1, and we can only be assured of linear response to μ for $\mu < T$.

With a few additional assumptions we can explore the behavior of the system for larger μ , when there is a free energy barrier. I will assume the free energy barrier is significantly

larger than T , and that the motion of N_{CS} is quite heavily damped, so that if one barrier is breached, enough of the energy used (and, at nonzero μ , gathered) in breaching it is lost that the system is unlikely to breach the next barrier before becoming thermalized in the new local minimum. In this case, the probability density will become equilibrated about the local minimum, and the probability to go over a barrier will be a kinetic prefactor, independent of μ , times the Boltzmann suppression to get to the top of the barrier. Here I tacitly assume μ is less than the barrier height, so the shape of the top of the barrier is not significantly modified. In this case, the rate of N_{CS} change will be

$$\langle \dot{N}_{CS} \rangle = V(\Gamma_{\text{forward}} - \Gamma_{\text{backward}}) \simeq \frac{\Gamma_d V}{2} \left(e^{\frac{-\mu}{2T}} - e^{\frac{\mu}{2T}} \right) = -\Gamma_d V \sinh \frac{\mu}{2T} \quad (17)$$

which of course has the correct small μ behavior. However, as μ becomes on order or greater than T , the rate rises, eventually greatly exceeding the linear extrapolation. The behavior will depart from the sinh function when the energy gained from the chemical potential in hopping a barrier becomes comparable to the loss from friction. Note that if, contrary to my assumption, the friction is weak, then most barrier jumping events are followed by another, and the diffusive motion will have very long time correlations. This is not observed in the simulations. I will just comment that, in this situation, the large μ behavior of the system again gives a rate which differs from the linear extrapolation by on order $\exp(\text{barrier height})$.

What happens when there is no barrier? I will mention the simplest possible model; that N_{CS} moves in a flat potential under a linear frictional force and a random force to keep it thermalized,

$$\ddot{N}_{CS} = -\gamma \dot{N}_{CS} + f \quad (18)$$

where f is independent of N_{CS} and has $\langle f(t)f(0) \rangle = 0$ for $t \neq 0$. Its magnitude is chosen so that N_{CS} will be thermalized at the correct temperature. Adding a chemical potential produces a term $-\mu N_{CS}$ on the righthand side. Averaging over realizations of f , the terms \ddot{N}_{CS} and f drop out of the determination of $\langle \dot{N}_{CS} \rangle$, which is strictly linear in μ . This behavior will eventually break down only because a realistic f does have a correlation time and a realistic friction is somewhat nonlinear and has some memory.

Now I will briefly discuss evaluating Γ_μ . It is a linear response coefficient, and as such we might expect that it can be computed from a correlator of the equilibrium theory. In fact this is the case (for the continuum theory); by considering modifying the Hamiltonian by $H \rightarrow H + \mu N_{CS}$ and applying the techniques of Kubo [14], we find

$$\Gamma_\mu = \lim_{t \rightarrow \infty} \frac{T \langle \{N_{CS}(t), N_{CS}(0)\} \rangle}{V}, \quad (19)$$

where $\{, \}$ are the Poisson brackets,

$$\{A, B\} = \sum_i \frac{\partial A}{\partial q_i(0)} \frac{\partial B}{\partial p_i(0)} - \frac{\partial B}{\partial q_i(0)} \frac{\partial A}{\partial p_i(0)}. \quad (20)$$

The derivatives in Eq. (19) are with respect to the coordinates and momenta at zero time. The poisson bracket we need then includes expressions such as $\partial N_{CS}(t)/\partial p(0)$. To evaluate numerically the contribution to this expression from one pair of conjugate variables in one representative configuration, we would have to make a small change to one momentum and

then evolve the system forward by time t , and compare N_{CS} to its value if we had performed the evolution without changing the momentum. Since we must sum over all coordinates and momenta (and on a lattice there are a great many) and over an ensemble of initial conditions, this will not be a very efficient way of measuring Γ_μ . A more practical way would be to perform all the terms in the sum on coordinates at once, by adjusting each coordinate and momentum according to the derivative of N_{CS} with respect to the corresponding momentum or coordinate. Provided that we make small changes, the final N_{CS} should depend linearly on each change, contributions arising because of the product of two of the changes we made being suppressed by a power of how small the changes were. We can also rely on the ergodicity of the system and apply the adjustments to coordinates and momenta at each time step, rather than at only one. This appears to be the only efficient way of evaluating Eq. (19); it is, however, equivalent to evaluating the evolution of the system under the action of the chemical potential. So we gain nothing by considering equilibrium correlators, and the best way to proceed numerically is to evolve the system with a chemical potential term added to the Hamiltonian.

3 The Model

Now I turn to the problem of how to measure Γ_μ . I will only be concerned with finding the high temperature limit. Far above the electroweak phase transition temperature the Higgs boson takes on a substantial plasma mass and probably does not influence the evolution of very infrared modes, so it will be sufficient to evolve the classical Yang-Mills field equations under the influence of a chemical potential for N_{CS} .

To prepare for the task I review the method of evolving the Yang-Mills equations when there is no chemical potential. The evolution of the fields is not completely specified by the field equations because they respect our freedom to choose a gauge; by specifying a gauge we render the evolution unique. The most convenient choice is the gauge which will make A_0 everywhere zero; in terms of the gauge fields A^i and their conjugate momenta, the electric fields E^i , and suppressing group indices, the continuum equations of motion in this gauge are

$$\begin{aligned}\frac{dA^i}{dt} &= E^i \\ \frac{dE^i}{dt} &= -D^j F^{ji}\end{aligned}\tag{21}$$

where F is the field strength tensor, and I have written the space components in terms of a positive three dimensional metric. In addition, the time component of the Yang-Mills equations of motion, which arises from minimizing with respect to variations in A_0 , enforces a first-class constraint,

$$D^i E^i = 0.\tag{22}$$

This Gauss constraint commutes with the equations of motion, so it need only be enforced on the initial conditions. However, it is important that this property be preserved numerically when we actually evolve the field equations.

It is also well known how to make a lattice version of the Yang-Mills field equations without a chemical potential [15]. The gauge fields become the link matrices U^i , and the electric fields are adjoint fields which I will take to lie at the beginning of each link, so the link update rule is

$$\dot{U}^i = E_\alpha^i i\tau_\alpha U^i. \quad (23)$$

(The left index of U lies at the beginning or basepoint of the link and the right index lies at the end. To parallel transport E_i to the end of its link, we then take $U_i^\dagger E_i U_i$.)

The Kogut-Susskind Hamiltonian is

$$H = \sum \frac{E_\alpha^i E_\alpha^i}{2} + \sum_{\square} 1 - \frac{1}{2} \text{Tr} U_\square \quad (24)$$

where the first sum is over all links and the second is over all elementary plaquettes, and U_\square means the product of the link matrices running around the plaquette. The coupling constant is absorbed into the inverse lattice temperature β_L which will be used to thermalize the system; with these conventions β_L corresponds to the continuum value $\beta_L = 4\beta_{\text{continuum}}/(g^2 a)$, a the lattice spacing.

The Gauss constraint at each lattice point is

$$\sum_i E_i(+) - E_i(-) = 0 \quad (25)$$

where $E_i(+)$ is the electric field on the link running forward out of the site and $E_i(-)$ is on the link running into the site from behind, parallel transported to the lattice site. This linear combination of E fields generates a gauge transformation of the U fields at the lattice point, and the requirement that it vanish can be understood as arising from our using up our freedom to make time dependent gauge transformations in choosing the temporal gauge. A simple leapfrog algorithm for the Kogut-Susskind Hamiltonian, as used in [8, 9], identically preserves the Gauss constraint. Krasnitz has recently developed an algorithm, based on a set of Langevin equations, for thermalizing this system to inverse temperature β_L while identically preserving the Gauss constraint; for details see [10].

To extract the value for Γ_d from the realtime evolution, one must keep track of the change in N_{CS} , which has a gauge invariant continuum definition, given in Eq. (3). In the leapfrog algorithm, where the U_i are defined at integer multiples of a time stepsize Δt and the electric fields live at half integer values, the simplest lattice realization which is invariant under the lattice point group is

$$\frac{\Delta N_{CS}}{\Delta t} = \frac{1}{2\pi^2} \sum_{\text{links}} \left(\frac{E_i^\alpha(t + \Delta t/2) + E_i^\alpha(t - \Delta t/2)}{2} \frac{1}{8} \sum_{8\square_i} \frac{1}{2} \text{Tr} - i\tau^\alpha U_\square \right), \quad (26)$$

where $8\square_i$ means a sum over the 8 plaquettes which begin and end at an endpoint of the link and run in the plane perpendicular to the link, see figure 1. (The factors of 2 differ from the continuum version because the lattice quantities are in terms of τ , while continuum fields are defined in terms of $\tau/2$.)

Now I will discuss the relationship of this model to the physical, quantum system we hope it will simulate. The degrees of freedom of the thermal, quantum Yang-Mills system fall into

3 categories. There are thermal energy particles with momenta characterized by the scale T , which interact very weakly with the other excitations, carry almost all of the energy of the system, and have ultrarelativistic dispersion relations. There are more infrared fields with momenta characterized by the plasma frequency $\sim gT$, which have substantial occupation numbers but interact perturbatively with the other degrees of freedom, except that forward scattering with the thermal particles make order unity modifications to their dispersion relations. And finally there are very infrared modes, with momentum characterized by the scale g^2T , with large occupation numbers and fully nonperturbative mutual interactions.

On the lattice there are also three characteristic scales: excitations with wavelength order the lattice spacing are weakly coupled, contain almost all of the system energy, and travel under the lattice dispersion relations; excitations of wavelength order a/β_L interact with each other nonperturbatively; and the intermediate scale again has perturbative interactions but dispersion relations substantially modified by interactions with the most energetic modes. The motion of N_{CS} in the symmetric electroweak phase depends on the most infrared modes. The idea of Grigoriev and Rubakov is that, in the quantum system these have such high occupation numbers that they should behave approximately as classical fields, and should therefore be correctly modeled by the classical lattice system[7]. If the high energy modes are only important as a thermal bath and for their corrections to dispersion relations, then the substitution of classical lattice modes for quantum continuum ones should not matter much.

Ambjorn and Krasnitz have also noted that the thermodynamics of the lattice model bears close resemblance to that of the full quantum system. In particular, if one introduces Lagrange multipliers A_0 to enforce the Gauss constraints and then performs the (Gaussian) integration over the electric fields, the partition function is almost the same as the partition function of the full theory, in the approximation of dimensional reduction [9, 16]. The difference is that the classical, lattice theory has zero *bare* Debye mass. However, a Debeye mass, linearly divergent in the lattice cutoff, is induced by the high energy excitations. Its value is [17]³

$$m_D^2(\text{lattice}) = \frac{4g^2\Sigma T}{4\pi a} \quad \Sigma = 3.1759114. \quad (27)$$

The lattice system therefore does in fact reproduce the thermodynamics of the full theory, for the right value of the lattice constant a . Yang-Mills Higgs theory has $m_D^2 = 5g^2T^2/6$, obtained in classical lattice Yang-Mills theory by $\beta_L \simeq 7.8$. The full standard model has $m_D^2 = 11g^2T^2/6$, corresponding to $\beta_L \simeq 17.2$. The independence of the rate Γ_d on β_L therefore indicates that Γ_d does not depend on the Debeye mass. I will return to this point in section 5. I will also discuss a potential problem, involving the functional form of the “hard thermal loops” induced by the high energy modes.

Now I turn to the problem of adding a chemical potential for N_{CS} . For the continuum equations of motion this is straightforward; one adds a term μN_{CS} to the Hamiltonian, and the evolution of A, E are modified by

$$\frac{dA^i}{dt} = \frac{dA^i}{dt}(\mu = 0) + \mu\{A^i, N_{CS}\} = E^i + 0\mu$$

³In that paper the coefficient is 5 rather than 4, because they work in Yang-Mills Higgs theory, and the interaction between A_0 and Higgs fields contributes 1 to the coefficient.

$$\frac{dE^i}{dt} = \frac{dE^i}{dt}(\mu = 0) + \mu\{E^i, N_{CS}\} = -D^j F^{ji} - \frac{\mu}{16\pi^2} \epsilon^{ijk} F^{jk} = -D^j F^{ji} - \frac{\mu}{8\pi^2} B^i \quad (28)$$

where $B^i = (1/2)\epsilon^{ijk} F^{jk}$ is the magnetic field in the i direction. Fortunately, for smooth fields

$$\epsilon^{ijk} D^i F^{jk} = 0 \quad (29)$$

by the Bianchi identity, and so the additional term still preserves the Gauss constraint.

An equivalent approach is to add to the action a term $\theta(t)\epsilon_{\mu\nu\alpha\beta} F_a^{\mu\nu} F_a^{\alpha\beta}$. If θ were a constant, then this term would be a total derivative and would not change the equations of motion; but if it varies in time, then when we integrate by parts in time while deriving equations of motion the time derivative acts on θ , generating the B^i term in the equations of motion. Proceeding in this fashion also makes it clear why the added term still commutes with the Gauss constraint; we should rederive the Gauss constraint with this added term in the action, but because the 0 index of the antisymmetric tensor is used up by A_0 , no time derivatives arise to act on θ , so the Gauss constraint is unchanged.

When we try to implement a chemical potential for N_{CS} on the lattice, we encounter trouble. The most obvious way is to find a lattice definition of N_{CS} and add it to the Hamiltonian. However, there is no lattice definition of N_{CS} which gives the desired behavior under gauge transformations. N_{CS} should be invariant under small gauge transformations and change by an integer under large ones; but on a lattice, a gauge transformation is a choice of one member of the gauge group at each lattice site, and since there are finitely many lattice sites and the gauge group $SU(2)$ is path connected, *any* gauge transformation can be built up infinitesimally. Therefore, either N_{CS} must be a constant, or it must vary continuously under gauge transformations. Also, we would like N_{CS} to change by the same amount on each application of the same gauge transformation; but any lattice N_{CS} is a function of finitely many variables, the U_i , which live on compact manifolds, and any continuous function on a compact domain is bounded. If it changed by some constant amount under a gauge transformation, then repeated application of the gauge transformation would drive it to infinity, a contradiction.

A second idea for implementing the chemical potential on the lattice [18] is to use this definition of the lattice $\epsilon^{\mu\nu\alpha\beta} F_{\mu\nu} F_{\alpha\beta}$ and the alternative implementation of the chemical potential in which we add $\theta(t)\epsilon^{\mu\nu\alpha\beta} F_{\mu\nu} F_{\alpha\beta}$ to the (lattice) action. The Gauss law, which is derived from the lattice action, is modified in a way such that it will be preserved by the new equations of motion.

This technique suffers from a new problem on the lattice, which is that the lattice definition of $\epsilon^{\mu\nu\alpha\beta} F_{\mu\nu} F_{\alpha\beta}$, Eq. (26), is not a total derivative. The simplest counterexample configuration contains just three non-identity link matrices; two, with values $1 + \epsilon i\tau_1$ and $1 + \epsilon i\tau_2$, lie on the two most removed links of a plaquette perpendicular to some link, and the third, with value $1 + \epsilon i\tau_3$, lies along the link, backwards one time step (see figure 2). The space integral of $\epsilon^{\mu\nu\alpha\beta} F_{\mu\nu} F_{\alpha\beta}$ for this configuration is nonzero even though all links at large distances are the unit link. The definition is therefore not a total derivative⁴. This is

⁴For any definition of the space integral of $\epsilon^{\mu\nu\alpha\beta} F_{\mu\nu} F_{\alpha\beta}$ which consists of a sum over lattice sites or links of some local gauge invariant operator, a similar counterexample can always be found; find three links which all appear in the evaluation of one, but only one, site or link, and shift their link matrices from the identity using three orthogonal Lie algebra elements; then they will contribute to $\int F\bar{F}$ at this point but not at any

a serious problem, because it means that even if θ is constant, the $\theta\epsilon^{\mu\nu\alpha\beta}F_{\mu\nu}F_{\alpha\beta}$ term will change the dynamics of the system; at late times θ will become large, and these (spurious) changes will actually dominate the dynamics.

We should not be too surprised that this technique did not work. The argument that $\epsilon^{\mu\nu\alpha\beta}F_{\mu\nu}F_{\alpha\beta}$ is a total derivative relied on the fields being smooth, a concept which is lost on the lattice, and its failure to be a total derivative explains why N_{CS} is not well defined. Recall that the chemical potential for N_{CS} emerged anyway by integrating out chiral fermions at nonzero chemical potential, and that it is impossible to implement chiral fermions on a lattice, a fact which may be related to our problems here.

Another idea, considered in [8], is to abandon the hope of deriving equations of motion from a Hamiltonian and to try to find a lattice implementation of the continuum equations of motion, Eq. (28). A natural choice for B_i is the average of the eight plaquettes used in Eq. (26); the equations of motion are then

$$\begin{aligned} U^i(t + \Delta t) &= \exp(i\Delta t\tau_\alpha E_\alpha^i)U^i(t) \\ E_\alpha^i(t + \Delta t/2) &= E_\alpha^i(t - \Delta t/2) - \sum_{4\square_i} \left(\frac{1}{2} \text{Tr}(-i\tau_\alpha)U_\square \right) - \frac{\mu}{16\pi^2} \sum_{8\square_i} \left(\frac{1}{2} \text{Tr}(-i\tau_\alpha)U_\square \right). \end{aligned} \quad (30)$$

Here $\sum_{4\square_i}$ means a sum over the 4 plaquettes which contain the link i , with orientation so as to contain U_i and not U_i^\dagger , and $\sum_{8\square_i}$ has the same meaning as previously. This technique is nice in that it corresponds to the physical meaning of a chemical potential term, that the E fields should be modified in accordance with the B fields so that the energy in the fields, $E \cdot E/2$, is modified by $E \cdot \delta E = -\mu\Delta t E \cdot B/(2\pi^2) = -\mu\Delta N_{CS}$.

The problem with this plan is that the evolution does not preserve the Gauss constraints, so we are exciting unphysical modes. Again, the nonabelian nature of the theory is essential; in the abelian theory, our definition of $\epsilon^{\mu\nu\alpha\beta}F_{\mu\nu}F_{\alpha\beta}$ is a total divergence, and the space divergence of the magnetic field at some point, which is the sum of all plaquettes on the surface of a box one lattice spacing around the point (see figure 3), is the boundary of a boundary, and vanishes identically, preserving the Gauss constraint. But in the nonabelian theory, while $D_i B_i$ is still the sum of all plaquettes around a cube, there are commutator terms which spoil the cancellation. That is, B_a^i is contaminated with nonrenormalizable operators such as $a^2 D^l D^l B^i$, and $D^i D^l D^l B^i$ need not vanish, since $[D^i, D^l]$ does not. Since the extra terms are nonrenormalizable, they will have vanishing influence on the infrared physics as the lattice spacing is made smaller; but if they introduce ultraviolet divergences in the measured value of Γ_μ then they will spoil the calculation.

If we ignore the violation of the Gauss constraint, or if we (dissipatively) remove the Gauss constraint violation occasionally or incompletely, we risk measuring changes in N_{CS} arising from the excitation of unphysical modes as well as from genuine topology change. The problem is that the combination of electric fields which produce a Gauss constraint violation has essentially no restoring force. If the chemical potential term causes this E field to change, then $E * B$ will be nonzero for the linear combination of E which make up the Gauss constraint; if there were a restoring force then E would oscillate and the time integral of $E * B$ would vanish, but instead E will rise and the integral need not vanish. If the Gauss constraint is dissipatively enforced occasionally, it is quite easy numerically to establish

other, and the definition will not be a total derivative. Note that the nonabelian nature of $SU(2)$ is essential.

how much of any accumulated N_{CS} corresponded to this process. Because of the chemical potential, the system energy shifts by $\mu\Delta N_{CS}$. Some of this energy goes into exciting Gauss constraint violations; the amount is μ times the amount of ΔN_{CS} which arose from exciting the unphysical modes. If the Gauss constraint violations are quenched, then the loss of energy in the quenching corresponds to the amount of spurious ΔN_{CS} . Numerically I find that this amount is a substantial share, if the Gauss constraint violation is only quenched occasionally. Further, a straightforward argument suggests that the problem should get worse as the lattice spacing is made smaller. In lattice units, in terms of the lattice inverse temperature β_L , the typical magnetic field strength is $B \sim \beta_L^{-1/2}$, and since the violation of the Gauss law depends on the nonabelian nature of the theory the size of the induced violation must go as $B \times B \sim \beta_L^{-1}$. To keep μ fixed in physical units as we change the lattice spacing, μ should go as β_L^{-1} , so the induced unphysical E field goes as $\mu B \times B \propto \beta_L^{-2}$ and the spurious energy introduced per unit lattice 4-volume goes as β_L^{-4} . The rate of N_{CS} violation per lattice 4-volume, for $\mu\beta_L$ fixed, due to genuine infrared topology changing processes should go as β_L^{-4} , and so the energy shift from these processes goes as β_L^{-5} . If this naive dimensional argument is right then, if the Gauss constraint is unquenched or poorly quenched, the contribution to Γ_μ due to excitation of the unphysical modes should grow linearly with inverse lattice spacing, and no fine lattice spacing limit for Γ_μ will be found.

The problem can be understood and cured by considering the implementation of the Hamiltonian equations of motion, Eq. (28), more carefully. When we modify the electric fields we should not modify all fields, but only the linear combinations orthogonal to those constrained to be zero. That is, the electric fields can be partitioned into two orthogonal subsets, the constraints $\{C^\alpha\}$ and the fields orthogonal to the constraints, which I call the E^* . At fixed U the E^* are in correspondence with the momenta of the canonical basis of the observable subspace. Only these E^* are dynamical, the C^α should be held zero. Since U is fixed during the update of E in the leapfrog algorithm, this means we should modify the update rule in Eq. (28) to

$$\begin{aligned}\frac{\Delta C^\alpha}{\Delta t} &= \frac{\Delta C^\alpha}{\Delta t}(\mu = 0) + 0 = 0 \\ \frac{\Delta E^*}{\Delta t} &= \frac{\Delta E^*}{\Delta t}(\mu = 0) + \mu\{E^*, NCS\}.\end{aligned}\tag{31}$$

This is exactly what we would conclude if we described ΔN_{CS} as $E^* \cdot B/(2\pi^2)$, which is of course equivalent to $E \cdot B/(2\pi^2)$, since the linear combinations of E orthogonal to all E^* are automatically zero.

We can implement this update by finding an orthonormal basis for the E^* ,

$$E_\alpha^* = \sum_i c_{\alpha i} E_i, \quad \sum_i c_{\alpha i} c_{\beta i} = \delta_{\alpha\beta}\tag{32}$$

and updating them by changing them by

$$E_\alpha^* = E_\alpha^* - \frac{\mu\Delta t}{2\pi^2} \sum_i c_{\alpha i} B_i\tag{33}$$

or

$$E_i = E_i - \frac{\mu\Delta t}{2\pi^2} \sum_\alpha c_{\alpha i} \sum_j c_{\alpha j} B_j,\tag{34}$$

which is basis independent and preserves the Gauss constraint by construction. Equivalently, given a complete orthonormal basis of Gauss constraints C_\perp^α ,

$$C_\perp^\alpha = \sum_i d_{\alpha i} E_i, \quad \sum_i d_{\alpha i} d_{\beta i} = \delta_{\alpha \beta} \quad \sum_\alpha c_{\alpha i} c_{\alpha j} + \sum_\beta d_{\beta i} d_{\beta j} = \delta_{ij}, \quad (35)$$

the update is

$$E_i = E_i - \frac{\mu \Delta t}{2\pi^2} \left(B_i - \sum_\alpha d_{\alpha i} \sum_j d_{\alpha j} B_j \right). \quad (36)$$

This technique as described is impractical. The problem is that (unlike in the abelian theory) the linear combinations E^* are in general not well localized and change with each time step. Finding them is a problem in the diagonalization of sparse matrices, but even if it could be performed efficiently, the number of operations required to implement Eq. (34) grows with the square of the number of lattice sites, which makes it numerically impractical. We also cannot implement the algorithm by using Eq. (36) because the natural, local basis for the Gauss constraints is not orthogonal, and again any orthogonal basis is not localized and changes with time.

However, there is a (linear in the number of lattice points) algorithm for implementing this update scheme approximately, which can be made highly accurate. The idea is that any update of form

$$E_i \rightarrow E_i - \frac{\mu \Delta t}{2\pi^2} \left(B_i - \sum_\alpha d_{\alpha i} \kappa_\alpha \right), \quad (37)$$

with $d_{\alpha i}$ describing any basis for the Gauss constraints, and with the κ_α completely arbitrary, will correctly modify the E^* . It is not even essential that the basis for the Gauss constraints be orthogonal, as long as it is complete, independent, and orthogonal to all E^* . What uniquely determines the right choices for the κ_α (once we have chosen a basis for the Gauss constraints and hence the $d_{\alpha i}$) is that the Gauss constraints must be satisfied at the end. If we can find an algorithm which, by only making changes to the E fields orthogonal to the E^* , incompletely but very accurately enforces the Gauss constraints at each step, and therefore picks almost the correct κ_α , then we will have almost the evolution of Eq. (34); and by improving the accuracy to which the Gauss constraints are approached we can test whether the results depend on the residual failure. This is the technique I will adopt for the evolution of the Yang-Mills system with a chemical potential. It is still not clear whether the failure to correctly simulate the ultraviolet physics will influence the resulting Γ_μ (although I will of course check if my results have sensible small volume behavior), but the infrared evolution should be correct, and no spurious physics should arise from violations of the Gauss constraints.

Restoring Gauss Constraints

I will now briefly describe two algorithms for the removal of the Gauss constraint violations. For the uninterested reader it is only necessary to know that algorithm 1 removes about half of the accumulated Gauss violation at each step, and algorithm 2 is about twice as costly in compute time, but leaves a residual Gauss constraint about one fifteenth as large.

The basic idea of quenching the Gauss constraint is to change the E field on a link in the direction which will reduce the Gauss violation at both endpoints. The most basic method is

$$E_i(x) \rightarrow E_i(x) + \gamma(U_i C(x + \hat{i}) U_i^\dagger - C(x)) \quad (38)$$

where by $C(x)$ I mean the Gauss violation at the point x , and I have of course parallel transported the forward C to the point where the group indices of E_i reside. This algorithm is equivalent to the relaxation algorithm with Hamiltonian $H = \sum_x C(x) * C(x)$ (Lie algebra dot product) used in [8], and it does not alter the E^* . Algorithm 1 is to apply this relaxation once at each timestep, using a value of γ chosen to make it efficient. To evaluate its efficiency it is useful to use Fourier analysis, which should be approximately valid in the ultraviolet (where most of the Gauss violation occurs). When $C(x) = C(k) \sin(k * x)$, each update takes

$$C(k) \rightarrow \left(1 - \gamma \sum_i 2(1 - \cos k_i)\right) C(k). \quad (39)$$

The sum is recognizable as $\omega^2(k)$ for the lattice dispersion relation, and its maximum value is 12. The sign of $C(k)$ oscillates with each application of the algorithm if $\gamma > 1/\omega^2(k)$, and if $\gamma > 1/6$ then the most ultraviolet mode becomes unstable. For γ close to 1/6 the damping becomes inefficient for the most ultraviolet modes. However, the damping of infrared modes is in general quite inefficient, and it is good to have γ as large as practical. Using $\gamma = 0.1$ or 0.12, I find the algorithm is quite efficient. If the algorithm is applied at each step, then the total Gauss violation, measured by $\sqrt{\sum_x C(x) * C(x)}$, after a step is about as large as the Gauss violation generated by one step, starting from no violation. For an 18^3 grid, a timestep of 0.06 lattice spacings, a chemical potential $\mu = 0.2$ in lattice units, and a lattice inverse temperature $\beta_L = 6$, I find $\langle C(x)_{rms} \rangle \sim 1.7 \times 10^{-4}$.

To determine how much of the accumulated N_{CS} in the realtime evolution of the lattice system was due to the Gauss constraint violation, I performed a linear regression fit of the energy of a lattice system to N_{CS} when the chemical potential term was turned on with $\mu = 0.2$ in lattice units, at $\beta_L = 5$ ($\mu = T$). The slope should equal μ if no Gauss constraint violations are generated; it was low by 7.5%, indicating that a nontrivial minority of the measured change in N_{CS} was due to the violation and subsequent quenching of Gauss constraints. When the algorithm was only applied every 16 steps, the slope was low by 37%. Clearly, then, quenching the Gauss constraints effectively makes a great deal of difference, but algorithm 1 is insufficiently thorough.

Algorithm 2 is a modification and improvement of algorithm 1. Because the time stepsize is by necessity much shorter than any frequency in the problem, the Gauss constraint violation generated at each time step will approximately equal that of the previous time step; a good first correction is to repeat some multiple $m < 1$ of the total modification made in the previous time step. Then one application of the relaxation algorithm described above is applied. This combination leaves an rms Gauss violation a factor of 4 smaller than algorithm 1. A further improvement is accomplished by applying the relaxation step twice each time step, with different stepsize constants γ_1 and γ_2 . All that is necessary for algorithm stability is that $1 > (1 - \gamma_1 \omega^2)(1 - \gamma_2 \omega^2) > -1/3$ (the lower bound would be -1 for $m = 0$, but changes when $m \neq 0$. The value I use is for $m = 1$.). By making the γ well separated, with $\gamma_2 > 1/6$, I make the algorithm efficient over a wide frequency range. I find that the

parameter choice $m = 0.9$, $\gamma_1 = 5/48$, and $\gamma_2 = 5/24$ gives excellent performance, with the Gauss constraint violation after application about 1/15 as large as with algorithm 1. Using this combination, the linear regression fit of energy versus N_{CS} gives μ to better than 1% for every lattice spacing used in this paper. I conclude that evolving the system using algorithm 2 is for all practical purposes equivalent to implementing Eq. (34). Incidentally I can also conclude that I implemented the chemical potential with the right numerical coefficient.

If it should prove necessary, it is straightforward to further improve algorithm 2; one repeats the relaxation step more than twice, with a different stepsize constant each time, chosen so that the function $\Pi(1 - \gamma_i \omega^2)$ will be as near zero in as wide a range as possible, and never outside the stability bound. For instance, I found that 3 applications with $\gamma = 7/72$, $7/48$, and $7/24$ leaves a residual violation about 2.5 times smaller than algorithm 2. Also, reducing the stepsize improves algorithm performance; algorithm 1 improves linearly with Δt and algorithm 2 (keeping $(1 - m)/\Delta t$ fixed) improves as the square.

4 Some Numerical Results

I implemented the Hamiltonian system with chemical potential described above, and the thermalization algorithm of Krasnitz[10]. The time stepsize for the Hamiltonian evolution was chosen as follows: in the ultraviolet (where most of the energy of the system resides) the Fourier modes behave as weakly coupled harmonic oscillators with frequency given by the lattice dispersion relation $\omega^2 = 2 \sum (1 - \cos k_i)$. Defining the energy of the system at time t to be

$$\text{Energy}(t) = \sum_{\square} 1 - \frac{1}{2} \text{Tr} U_{\square}(t) + \sum \frac{E^2(t + \frac{\Delta t}{2})}{4} + \sum \frac{E^2(t - \frac{\Delta t}{2})}{4}, \quad (40)$$

the leapfrog algorithm should keep the central value of energy stable for a harmonic oscillator, but the amplitude of oscillations in the energy of a harmonic oscillator should be $\omega^2 \Delta t^2 / 4$ times the energy. To keep these fluctuations at most 1% for the most ultraviolet mode ($\omega^2 = 12$) it is necessary to choose $\Delta t \leq 0.06$. I choose $\Delta t = 0.06$ in all simulations discussed in this paper. Integrating over all the modes, the perturbative estimate of the variance in the energy of an N^3 lattice at lattice inverse temperature β_L , in the limit of large N , is

$$\sigma_{\text{Energy}}^2 \simeq (N_{\text{DOF}}) \langle (E_{\text{DOF}}^2) \rangle \frac{\langle \omega^4 \rangle (\Delta t)^4}{32} = 6N^3 \frac{2}{\beta_L^2} \frac{213}{8} \frac{(\Delta t)^4}{32} \simeq 1.29 \times 10^{-4} \frac{N^3}{\beta_L^2} \quad (41)$$

for my value of Δt . The energy of the system without chemical potential was in fact absolutely stable to overall drift, with variance within 10% of the analytic estimate, for runs on large and small lattices. I also checked that, for initial conditions with only one excited mode, the dispersion relations were correct.

To test the thermalization algorithm I measured the overall energy and compared it to $6N^3/\beta_L$, which is the free field estimate (there are 6 degrees of freedom per site); it agreed to a few percent, better at large β_L and worse at low β_L . I also compared the values of Wilson loops to the results of Krasnitz[10], and found good agreement.

A more substantive check was to measure the N_{CS} diffusion rate in the absence of a chemical potential for a thermalized system, comparing to the results of Ambjorn and Kras-

β_L	3	4	5	6	7	8
$\kappa_{d,t=\beta_L\pi}$.48 \pm .04	.71 \pm .06	.93 \pm .09	1.16 \pm .10	1.07 \pm .10	1.14 \pm .12
$\kappa_{d,t=2\beta_L\pi}$.49 \pm .06	.67 \pm .08	.93 \pm .13	1.08 \pm .13	1.04 \pm .14	1.30 \pm .20

Table 1: Values of κ_d , the dimensionless Γ_d , for various inverse lattice spacings. All data-points are for lattices of size $N = 3\beta_L$ to prevent finite volume effects. Finite spacing effects become important around $\beta_L = 5$.

nitz. Because my computer resources were limited I could not check their results at the large values of β_L they used; instead I measured Γ_d at a range of smaller β_L , to find at what value lattice coarseness effects arise. I was also unable to demonstrate in a convincing way that the ultraviolet, white noise fluctuations satisfy their analytic estimate of $\delta N_{CS}^2 = 0.00684N^3/(\pi\beta_L)^2$; instead I assumed this behavior and subtracted it off from the value of $(N_{CS}(t) - N_{CS}(0))^2$; however I compare two values of t to check the validity of this procedure. Expressing $\Gamma_d = \kappa_d/(\beta_L\pi)^4$, (this value of κ corresponds to the value defined in the introduction), I present my values for κ_d in Table 1. All error bars are one σ and statistical.

It is clear from the table that values of $\beta_L \leq 5$ are contaminated with some finite lattice spacing effect, but the results above this scale are consistent with those of Ambjorn and Krasnitz.

Next I implemented the chemical potential on the lattice, as described in the previous section. As a first check to see whether the technique will be plagued with ultraviolet divergences, I thermalized the system so that all U and E would fall in an abelian subspace of $SU(2)$ and its Lie algebra. This is easy to do with the thermalization algorithm of Krasnitz, because initial conditions which only contain excitation in one Lie algebra direction never have the other Lie algebra directions excited by the algorithm. The evolution is then equivalent to compact $U(1)$ gauge theory, in which N_{CS} should oscillate about 0 but never drift. Indeed, when I applied a chemical potential, the value of N_{CS} did not drift, but fluctuated in a narrow range about 0; so if there are ultraviolet problems in the chemical potential method, they only arise out of nonabelian interactions.

As a next test of the reliability of the algorithm I measured $\langle \dot{N}_{CS} \rangle$ with $\mu = 1/\beta_L$, which should give half $\Gamma_d V$. I will express my results as $\kappa(\mu\beta_L) \equiv \langle \dot{N}_{CS} \rangle (\beta_L\pi)^4/(\mu\beta_L N^3)$; we should expect $\kappa(\mu\beta_L) = \kappa_d/2$ for small $\mu\beta_L$. I find that, for $\beta_L = 5$, $\kappa(1.0) = .46 \pm .03$; for $\beta_L = 6$, $\kappa(1.2) = .50 \pm .04$; and for $\beta_L = 8$, $\kappa(1.0) = .60 \pm .11$. All three results are on lattices of length $N = 3\beta_L$, well larger than the size Ambjorn and Krasnitz found would remove finite scaling effects. These results are in very good agreement with the measured values of κ_d , and same trend in β_L , which is suggestive that both techniques are working correctly.

However, since the implementation of the chemical potential, while probably correct for infrared excitations, is almost certainly wrong for ultraviolet excitations at the lattice scale, it is a good idea to test the finite volume behavior of the results. We expect that, when the volume of the lattice is made small, there will not be enough room for energetically unsuppressed topology changing events, which must be spatially extensive, to exist, and the rate of topology change should fall. If our results arise from true infrared behavior then we should see $\kappa(\mu\beta_L)$ fall; but if our results arise from spurious ultraviolet effects, then the rate

N	N/β_L	$\kappa(1.2)$
4	.67	.15 \pm .04
6	1.0	.19 \pm .05
8	1.33	.41 \pm .07
12	2.0	.49 \pm .06
18	3.0	.50 \pm .04
24	4.0	.53 \pm .06

Table 2: Dependence of $\kappa(\mu\beta_L)$ on lattice volume for $\beta_L = 6$. The rate of topology change is clearly suppressed on small volumes and saturates around $N = 2\beta_L$. Error bars are statistical and 1σ .

should simply scale with the 4-volume of the simulation and $\kappa(\mu\beta_L)$ should be unchanged.

I measured $\kappa(\mu\beta_L)$ for $\mu\beta_L = 1.2$ and $\beta_L = 6$ for a number of lattice sizes. The results are presented in Table 2 and Figure 4. Each datapoint represents a total lattice 4-volume of about $2 \times 10^7 a^4$ (a the lattice length). It is clear that the rate is falling for small lattice size, and the curve is about the same as that found by Ambjorn and Krasnitz for κ_d . Hence we can conclude that the results are in fact due to infrared physics, which the model should treat properly.

With the algorithm thus tested, I can now investigate a new question; what is the behavior of the system under large chemical potentials $\mu \gg 1/\beta_L$? This directly tests whether there is a free energy barrier to the flow of N_{CS} , as I discussed in section 2. Again, I use $\beta_L = 6$ in a compromise between compute time (which goes as β_L^4) and lattice refinement. I present some results in Table 3 and plot them in Figure 5. For the larger values of μ it was necessary to correct for the finite heating of the system, and to use several short evolutions of independent thermal initial conditions to minimize the amount of heating. The data show that $\langle \dot{N}_{CS} \rangle$ rises almost linearly with μ up to $\mu\beta_L \geq 6$, in stark contrast to the behavior when there is a free energy barrier. The errors quoted are all statistical, but there may be common systematic errors at the level of 3% from thermalization and finite stepsize. I also measured $\langle \dot{N}_{CS} \rangle$ for $\beta_L = 10$, $\mu\beta_L = 10$, and $N = 30$ and found $\kappa(10) = .607 \pm .022$, which shows that the approximate linearity is not a small β_L artefact, but that the slight departure from linearity (the excess of $\kappa(10)$ over $\kappa(1)$), is also probably real.

5 Modified Lattice

There is one potential problem with the classical lattice technique which might mean that the results for Γ_d and Γ_μ do not correspond to the correct continuum, quantum behavior. While the thermodynamic properties of the lattice system may be the same as the continuum theory in the infrared (in the very good approximation of dimensional reduction for the continuum theory), the dynamics may be different; in particular, while we know that the “hard thermal loop” corrections to the static propagator, namely the Debye screening, are of the same functional form as in the quantum system, this does not extend to the nonzero frequency case. Bodeker et. al. have recently shown that, because the most ultraviolet modes move under lattice rather than ultrarelativistic dispersion relations and have a rotationally noninvariant

N	$\mu\beta_L$	$\langle \dot{N}_{CS} \rangle (\beta_L \pi)^4 / N^3$	$\kappa(\mu\beta_L)$
18	0.5	.29 \pm .08	.58 \pm .16
18	1.2	.60 \pm .05	.50 \pm .04
18	2	1.15 \pm .09	.57 \pm .05
18	3	1.34 \pm .09	.45 \pm .03
18	4	2.01 \pm .09	.50 \pm .02
18	5	2.53 \pm .09	.51 \pm .02
18	6	2.92 \pm .13	.49 \pm .02
18	7	3.66 \pm .13	.52 \pm .02
18	8	4.19 \pm .13	.52 \pm .02
18	9	4.81 \pm .14	.54 \pm .02
18	15	8.93 \pm .30	.60 \pm .02
18	16	9.76 \pm .40	.61 \pm .02
18	18	10.0 \pm .4	.56 \pm .02
18	20	11.38 \pm .46	.57 \pm .02
18	22	13.1 \pm .5	.60 \pm .02
18	24	14.9 \pm .6	.62 \pm .02

Table 3: Rate of N_{CS} change as a function of chemical potential. The rate is surprisingly linear, but turns up somewhat for $\mu\beta_L \geq 10$. Error bars are statistical and 1σ .

ultraviolet cutoff, they induce corrections in the propagators of the intermediate scale which are not the same as the “hard thermal loop” effects of the quantum theory, and are in fact not even rotationally invariant [19]⁵. This sort of cutoff dependence is typical of linearly divergent quantities. While the lattice coarseness independence of Γ_d demonstrates that the overall magnitude of the “hard thermal loop” effects does not matter (at least when the lattice is fine enough that the Debeye screening scale and the nonperturbative scale are well separated), it is possible that the detailed \vec{k}/k_0 dependence of these corrections matters in the determination of Γ_d . This possibility is motivated by Braaten and Pisarski’s calculation of the gluon damping rate, in which the magnitude of the plasmon mass (proportional to the strength of hard thermal loop effects) cancels out, but the functional form of the hard thermal loops determines the calculation[20].

A related but less urgent matter is to understand why Γ_d falls as the lattice becomes quite coarse. There are two possibilities for this behavior. One is that the lattice is incorrectly evolving the infrared equations of motion due to artefacts, namely nonrenormalizable operators induced by the crude choice of lattice action. As the lattice becomes finer the effect of these artefacts on the behavior of the nonperturbative infrared modes falls as β_L^{-2} . Another possibility is that Γ_d is only constant in the limit that the nonperturbative length scale ($O(\beta_L)$ in lattice units) and the Debeye screening length scale ($O(\beta_L^{1/2})$ in lattice units) are well separated.

One can study at least the first of these issues by the following technique. I design a lattice action which has different (wrong) ultraviolet dispersion relations and will induce

⁵In fact Bodeker et. al. show this explicitly only for the abelian Higgs theory, but there is no reason to doubt that the same thing happens in Yang-Mills theory as well.

Hamiltonian	β_L	N	$\mu\beta_L$	κ
new	3.0	9	3.0	.177 \pm .011
new	4.0	12	3.0	.281 \pm .021
new	5.0	15	3.0	.302 \pm .032
new	6.0	18	3.0	.357 \pm .030
new	8.0	24	5.0	.393 \pm .034
new	10.0	30	10.0	.585 \pm .022
old	10.0	30	10.0	.607 \pm .022

Table 4: N_{CS} violation rate for Hamiltonian including rectangular plaquettes. All volumes are large enough to eliminate finite volume effects. The rate begins to scale with lattice coarseness more slowly reaches the same limit, as shown in the last column.

different (wrong) hard thermal loops. Then I measure $\kappa(\mu)$ for different lattice coarsenesses and see if there is a large lattice size limit and whether it is the same as the limit for the normal cubic lattice action. If it is, then the limit did not depend on which (wrong) hard thermal loops were induced, and would presumably not change if the right hard thermal loops could be induced.

I examined two modifications of the lattice action. In the first, I make the spatial part of the Hamiltonian $5/3 \sum_{\square} (1 - 1/2 \text{Tr} U_{\square}) - 1/12 \sum_{\square\Box} (1 - 1/2 \text{Tr} U_{\square\Box})$, where the second sum is over all 1×2 rectangular plaquettes (both orientations). This choice gives steeper dispersion relations in the ultraviolet. For modes with $\partial_1 E_1 = \partial_2 E_2 = \partial_3 E_3 = 0$ the expansion of ω^2 in k has no quartic term; but for other modes it has positive $k_1^2 k_2^2$ type terms, and the action is not an “improved” action in the sense of eliminating dimension 6 operators from the Hamiltonian⁶.

I analyzed this model for several lattice coarsenesses (values of β_L), generating the initial conditions with the thermalization algorithm discussed in Appendix A. Because the Hamiltonian is more complicated, the numerics were more time consuming; to get good statistics I was forced to assume that $\langle \dot{N}_{CS} \rangle$ rises linearly with μ up to $\beta\mu \simeq 5$, rather than verifying it explicitly as I did for the standard Hamiltonian. Some results are presented in Table 4. The same scaling behavior is reached, although the lattice must be finer before it is attained. It is not clear whether the approach to scaling is slower because the Debeye mass is smaller at the same β_L (it depends on the integral of ω^{-2} , and ω is larger in the ultraviolet in this model), or because of the different dimension 6 artefacts.

An alternate and stronger check is to deliberately make cutoff scale lattice behavior even worse, so the hard thermal loops will look even less like their correct values. If the small lattice size limit is unaffected then there can be little doubt that the functional form of the hard thermal loops really is not important.

To do this I make one lattice direction longer than the other two. That is, defining the

⁶The easiest way to see this is to consider the thermodynamics of the model; introduce Lagrange multipliers $A_0(x)$ for the constraint at site x and perform the Gaussian integration over the fields E . This generates a kinetic term for A_0 which is precisely the minimal (unimproved) implementation of $(D_i A_0)^2/2$. An improved action should produce an improved kinetic term for A_0 .

electric field E by $U(t + \Delta t) = \exp(i\Delta t \tau \cdot E)U(t)$, I take as my dot product

$$A \cdot B = \sum_{\text{sites}} l(A_1 B_1 + A_2 B_2) + l^{-1} A_3 B_3, \quad (42)$$

as my Hamiltonian

$$H = \frac{E \cdot E}{2} + \sum_{\square} l \left(1 - \frac{1}{2} \text{Tr} U_{\square_{12}} \right) + l^{-1} \left(1 - \frac{1}{2} \text{Tr} U_{\square_{13}} + 1 - \frac{1}{2} \text{Tr} U_{\square_{23}} \right), \quad (43)$$

as my magnetic fields

$$\begin{aligned} 8B_1^a &= l^{-1} \sum_{8\square} \frac{1}{2} \text{Tr}(-i\tau^a) U_{\square_{23}}, \\ 8B_2^a &= l^{-1} \sum_{8\square} \frac{1}{2} \text{Tr}(-i\tau^a) U_{\square_{31}}, \\ 8B_3^a &= l \sum_{8\square} \frac{1}{2} \text{Tr}(-i\tau^a) U_{\square_{12}}, \end{aligned} \quad (44)$$

as my definition of $D_j F_{ji}$

$$\begin{aligned} (D_j F_{j1})_a &= l^{-2} \sum_{\square_{13}} \frac{1}{2} \text{Tr}(-i\tau_a) U_{\square_{13}} + \sum_{\square_{12}} \frac{1}{2} \text{Tr}(-i\tau_a) U_{\square_{12}} \\ (D_j F_{j2})_a &= l^{-2} \sum_{\square_{23}} \frac{1}{2} \text{Tr}(-i\tau_a) U_{\square_{23}} + \sum_{\square_{12}} \frac{1}{2} \text{Tr}(-i\tau_a) U_{\square_{12}} \\ (D_j F_{j3})_a &= \sum_{4\square} \frac{1}{2} \text{Tr}(-i\tau_a) U_{\square}, \end{aligned} \quad (45)$$

(where the orientations should be taken as appropriate), and as my ΔN_{CS}

$$\Delta N_{CS} = \frac{E \cdot B \Delta t}{2\pi^2}. \quad (46)$$

The update rules for U and E are, in terms of B and $D_j F_{ji}$ defined above, unchanged. The thermalization algorithm and the Gauss law restoration are discussed in Appendix A. The thermalization is applied so that the total energy will be $6lN^3/\beta$ (6 the number of degrees of freedom).

To determine how we should expect this modification to change the observed rate of N_{CS} violation, it is simplest to successively stretch each lattice direction by the same factor of l . The resulting model is the same as the original cubic lattice model, except for factors of l . The energy in the magnetic field goes as $l^{-1} \sum_{\square} 1 - 1/2 \text{Tr} U_{\square}$, but its magnitude grows as l^3 ; so the magnitude of $1 - 1/2 \text{Tr} U_{\square}$ has grown as l^4 . Therefore the new model corresponds to the old model with β_L divided by l^4 . Also, because the expectation value of E only grows as l and not l^2 , we find that the time step has changed by a factor of l^{-1} . The chemical potential, in lattice units, is unchanged. Therefore, the expected value of $\langle \dot{N}_{CS} \rangle$ should change as the $4 * 3 - 1 = 11$ power of l , and stretching only one direction by l , using the definition of the system discussed above, should change the rate by $l^{11/3}$. To compensate, I shift my value of

β_l	N	l	$\beta\mu$	$\kappa(\mu)$
5.45	24	1.33	4	.56±.03
6.70	24	1.14	4	.50±.04
8.00	24	1.50	6	.73±.05
8.00	24	1.50	3	.67±.05
8.00	24	1.40	6	.64±.04
8.00	24	1.30	6	.64±.04
8.00	24	1.00	4	.57±.05
8.00	24	0.80	6	.57±.04
8.00	24	0.70	6	.54±.04
8.00	24	0.60	6	.55±.04
9.36	24	0.88	4	.65±.07
10.77	24	0.80	4	.47±.08
12.23	24	0.73	4	.60±.10

Table 5: An assortment of data on an elongated lattice. There is no strong trend, although the very large l points turn up.

β_L by $l^{-4/3}$ and my value of Δt by $l^{1/3}$; I should then expect the rate to be l independent, as long as β_L is large enough to eliminate finite spacing artefacts and N is large enough to eliminate finite volume artefacts. Because the grid is rectangular, these are more stringent conditions than in the cubic lattice case.

I have tested the behavior of this stretched lattice for several values of l , choosing β_L (including the $l^{-4/3}$ correction) to be around 8. Some results are presented in Table 6. The data suggests a very weak dependence on l , with the rate rising slightly for quite high values. This suggests some weak lattice shape dependence, presumably arising from a weak dependence on the hard thermal loops, but the effect is small and it is reasonable to believe based on this evidence that the value for κ determined from the cubic lattice should be quite close to the value we would find if we could include the right hard thermal loops.

6 $SU(3)$

The topological structure which exists in $SU(2)$ (weak isospin) gauge theory also exists for $SU(3)$ (color); there is a Chern-Simons number, and at high temperatures, thermal excitations should be the dominant means of topology change[21]. The rate of these changes, Γ_{strong} , is another important quantity to baryogenesis, since it may control the rate at which fermions change chirality in the plasma[22]. Parametrically, the N_{CS} diffusion rate can be written as $\Gamma_{d,strong} = \kappa_{d,strong}(\alpha_s T)^4$, with the constant $\kappa_{d,strong}$ another unknown.

The rate can be measured by a straightforward extension of the chemical potential method used for $SU(2)$. Group and Lie algebra elements should be chosen from $SU(3)$ rather than $SU(2)$, and $1 - 1/2\text{Tr}$ should be replaced by $3/2 - 1/2\text{Re Tr}$; with these substitutions everything carries over. The lattice inverse temperature is now related to the physical temperature as $\beta_L = 4\beta_{continuum}/(g_s^2 a)$, which will generate the correct power of g_s ; the constant $\kappa_{d,strong} = 2\kappa_{\mu,strong}$ can be gotten from simulations in the same way as κ_μ . The ther-

β_L	N	Energy/($16N^3/\beta_L$)	$\mu\beta_L$	$\kappa_{strong}(\mu)$
3	9	1.09	3	0.52 ± 0.05
4	12	1.10	4	1.19 ± 0.06
5	15	1.09	5	1.87 ± 0.09
6	18	1.07	6	2.30 ± 0.11
7	18	1.05	5	3.01 ± 0.19
10	24	1.035	6	3.19 ± 0.25
12	24	1.032	8	3.86 ± 0.30
14	28	1.025	6	4.26 ± 0.45

Table 6: Rate of topology change in $SU(3)$ lattice gauge theory at various lattice refinements. It is not clear that the fine lattice limit is reached, even at twice the refinement necessary in the $SU(2)$ case.

malization algorithm, presented in Appendix A. also carries over to $SU(3)$ without serious modification.

In practice, because the group $SU(3)$ is larger than $SU(2)$, and because the anticommutators of the Lie algebra generators λ_a are not multiples of the identity element, it is much more numerically costly to simulate the group $SU(3)$; I find that the time to update a lattice of the same size is approximately 8 times larger for $SU(3)$ than for $SU(2)$. Also, I find that the required inverse lattice spacing β_L must be larger before the results become β_L independent. Because of these complications, I was unable to verify that \dot{N}_{CS} rises linearly with μ . Instead, I have assumed that this behavior carries over from the $SU(2)$ case. I can then use quite a large value for $\mu\beta_L$, which is necessary to get good statistics out of relatively short runs. (The length of a run necessary to get fixed statistical error scales as the square of μ .) Unfortunately, this introduces a possible systematic error; it can be eliminated only with a great deal more computer time.

I have also been unable to check explicitly that the rate displays similar lattice volume behavior to the $SU(2)$ case; instead I have assumed that the rate becomes volume independent on lattices with $N > 2\beta_L$. Since the magnetic screening length of $SU(3)$ is presumably shorter than that for $SU(2)$, this assumption is almost certainly justified.

I present some numerical results for $\kappa_{\mu, strong}$ in Table 6. Because of the limitations discussed above, these should be considered preliminary; the systematic error bars are probably at least 10%. A preliminary estimate for the ratio $\kappa_{\mu, strong}/\kappa_\mu$ is 7 ± 1 , but it is not clear from the data whether the finest lattice used was large enough to reach the fine lattice limit.

Note also that the energy is systematically higher than the leading order perturbative estimate (the number of degrees of freedom divided by β_L). This effect is real. Since the electric fields appear quadratically in the Hamiltonian, I can compute that the energy in E fields should be $8N^3/\beta_L$, and this is satisfied numerically. The same energy excess in the magnetic fields was observed in $SU(2)$; for $SU(3)$ it is more than twice as large, presumably because there are more ways for the fields to interact.

7 Conclusion

It is possible to include a chemical potential for N_{CS} in lattice simulations of the classical Yang-Mills field equations, and the rate of N_{CS} motion is related to that of N_{CS} diffusion in the manner demanded by the detailed balance argument. Furthermore, the results show that there is no free energy barrier to topology change in the symmetric phase, because the response of N_{CS} grows linearly with chemical potential over a much wider range than is possible if the transitions occur by hopping over a barrier. I have also demonstrated that the classical, lattice rate is weakly, if at all, dependent on the details of the hard thermal loops induced by the high momentum modes.

To conclude, I will mention a possible interpretation of the results, and some directions for future work.

The two striking things about the rate of N_{CS} change under a chemical potential are that, in terms of the volume necessary to remove finite size effects, the rate seems very low, and that the rate remains linear up to surprisingly large values of chemical potential μ . These two things may be related. Consider a square Wilson loop of length x on a side in the continuum limit of the classical theory. When $x \ll \beta$ (by which I mean $a\beta_L$ as we take β_L to infinity and a to zero) the trace of the loop is $2(1 - Cx/(2\beta))$, where

$$C = \frac{n^2 - 1}{2\pi^2} \int dk_1 dk_2 \frac{1 - \cos(k_1)}{k_1^2} \frac{1 - \cos(k_2)}{k_2^2} \sqrt{k_1^2 + k_2^2} \quad (47)$$

for $SU(n)$ gauge theory. This expression has an ultraviolet logarithmic divergence, but what I am interested in is the contributions from $k \sim \pi/a$, which are $O(1)$, with no powers of π . The length scale where the “correction” term which makes the trace $\neq 2$ becomes order 1, which is the scale where nonperturbative physics sets in, is $x \sim \beta_L$, with no powers of π . This is the length scale where excitations no longer remain coherent long enough for energy to oscillate between E and B fields, and it is reasonable to expect, then, that it is the scale where \dot{N}_{CS} will lose its oscillatory behavior and behave in a Brownian fashion. The characteristic 4-volume of Brownian motion is thus $O(\beta^4)$, with no powers of π , which corresponds to the minimum volume for finite volume effects to disappear, and the magnitude of $E \cdot B$, integrated over one such 4-volume, is $O(1)$, again with no powers of π . To get $\delta N_{CS} = E \cdot B / (2\pi^2)$ to be $O(1)$ then requires $O(\pi^4)$ characteristic Brownian motion 4-volumes, and we should anticipate $\Gamma \sim (\pi\beta)^{-4}$, not β^{-4} , or $\kappa_d \sim 1$, not $\sim \pi^4$.

Turning to the chemical potential, one would expect that μ would start seriously changing the dynamics of the infrared when $\mu E \cdot B / (2\pi^2)$, integrated over a volume of order β^4 , is order β^{-1} , that is, when $\mu\beta \sim \pi^2$; and that for values smaller than this, the chemical potential is a small correction to the dynamics and the response should be linear. Again, this corresponds well to the actual behavior of the system.

What possible future projects can the chemical potential method be applied to? One question I could not answer here was whether the N_{CS} diffusion rate falls off on coarse lattices because the Debye screening length comes on order the scale of nonperturbative infrared physics, or whether it represents the effects of nonrenormalizable operators arising from the crudeness of the lattice action. One could resolve this question by finding a lattice Hamiltonian system and an update algorithm which do not generate dimension 6 nonrenormalizable operators in the infrared physics. If dimension 6 nonrenormalizable operators

are causing problems on coarse lattices then such a program could also allow better study of the $SU(3)$ case without requiring the very fine lattices which make such study numerically expensive. Also, knowing whether or not Debeye screening is important would help to clarify the role which hard thermal loops play in the calculation.

Also, extending the “chemical potential method” to the Yang-Mills Higgs theory allows one to study the out of equilibrium decay of the infrared gauge fields as they are swept up a bubble wall during the electroweak phase transition. It is frequently assumed in the literature that any left handed baryon number asymmetry generated by the motion of the bubble wall must find its way to the symmetric phase to cause baryon number generation, because N_{CS} violating processes are exponentially suppressed in almost all of the wall and in the broken phase[23]; and a contrary assumption, that a chemical potential for N_{CS} present on the wall can act on the infrared gauge field configurations as they decay[24], has never been convincingly tested. The method proposed here could be used to do so, for instance by integrating out the fermions analytically to produce effective interactions in the two doublet model, and numerically evolving the system through the electroweak phase transition.

Acknowledgements

I would like to thank A. Krasnitz for sparking my interest in this topic, and for useful conversations and criticism, and Neil Turok and Chris Barnes, for stimulating discussions. I would also like to thank Carl Edman, for donating a great deal of computer time.

8 Appendix A

In this appendix I present a simple, efficient thermalization algorithm for the classical lattice Yang-Mills or Yang-Mills Higgs system, or for any system in which the phase space is a vector bundle over the space of coordinates, with a Hamiltonian which is a pure coordinate term plus an inner product on the vector space, with the inner product allowed to be coordinate dependent. Constraints on the momenta are permitted provided they are linear, ie in each vector space they restrict to a vector subspace. (In the case of Yang-Mills theory the phase space is the tangent bundle over the space of U , and the constraints restrict the momentum vector to have a zero projection in each direction which corresponds to a gauge transformation on the space of U .) The algorithm is faster than that of Krasnitz, and much easier to apply to new systems, although the above requirements make it less general. Almost all the numerical equipment it uses must be developed anyway for the evolution of the system with a chemical potential.

The idea is the following; we begin in the vacuum. Then we fully thermalize the E fields, leaving the link matrices U untouched. That is, we draw E with correct Boltzmann weight from the vector space of allowed E at that value of U . We then evolve the fields according to the classical Hamiltonian equations of motion, allowing the thermalization to mix between E and U fields. Then we throw out the values of the E fields and fully rethermalize them; we repeat the thermalization and evolution over and over until the system is completely thermalized.

Now suppose there is an ensamble of systems described by some probability distribution, and consider how it evolves under this algorithm, averaging over realizations of the

algorithm. If we really draw E with correct thermal weight from the fixed U fiber, then the correct thermal probability distribution will be preserved by the algorithm. Further, any probability distribution preserved by the algorithm must have the property that the probability distribution is a product of a function on the coordinate manifold and a function on each fiber, with the function on each fiber the thermal distribution for the E fields at that value of U ; and this property must be preserved by the Hamiltonian evolution. Only the correct thermal distribution satisfies these conditions. Hence the algorithm should be correct. The only problem is finding a way to draw E from the thermal distribution on a fiber.

Now the thermal distribution function on the fiber of a particular U (that is, on the space of E at fixed U) is Gaussian. All we have to do to thermalize the E fields in this vector space is draw a value from the Gaussian distribution. In the absence of constraints, this would be easy. The problem is that, in the obvious natural basis for the E fields, the constraints are very nontrivial linear combinations of E fields, and to find an orthonormal basis of the directions in the dynamical subspace (the subspace permitted under the constraints) we must diagonalize a large matrix, as discussed in section 3. However, this does not turn out to be a fundamental problem.

The key is to notice that the obvious basis of E fields is orthonormal (up to a factor of 2) under the inner product defined by the Hamiltonian. If we choose each E field independently from the Gaussian distribution, then that will also choose the fields independently from the Gaussian distribution in any other orthonormal basis for the E fields, a special property of the Gaussian distribution. This includes any basis which decomposes into a subset $\{E^*\}$ orthogonal to the constraints and a subset $\{C_\perp^\alpha\}$ along constraint directions. This means that we will have chosen the E^* correctly. All that remains is to set the C_\perp^α to zero without changing the E^* , that is, to orthogonally project to the constraint subspace. But I have already presented a dissipative algorithm for doing so; by applying the dissipation step repeatedly, we can quite easily bring the magnitudes of the Gauss constraint violations to the level of machine roundoff accuracy. The electric fields are then correctly thermalized.

I should comment that the demands on the dissipative algorithm here are different from the demands during the evolution of the fields with chemical potential; so the optimal values of the algorithm coefficients are quite different. I find that, for algorithm 2, the value of m should be brought down to $m \sim 0.5$ or 0.6 .

I implemented this algorithm for the Yang-Mills system and compared it to the algorithm of Krasnitz[10]; I used the stepsize $\Delta t = 0.03$ in lattice units for my algorithm and $\Delta t = \gamma_E = 0.03$ for the algorithm of Krasnitz. I used 10 E field randomizations with evolutions of length β_L between them for my algorithm. On lattices of $N = 15$ and $N = 18$ I systematically found my algorithm gave total energies about 1% less than the algorithm of Krasnitz; this is probably because of the rather large time step and dissipation constant I used to implement his algorithm. (In his paper he advocates a more conservative stepsize.) I also compared the values of Wilson loops and found them to be within the same 1% margin. That their values are preserved by the Hamiltonian evolution of the thermalized system, is more or less automatic in my algorithm; but I tested it anyway and found it was true.

It is completely straightforward to extend this algorithm to the group $SU(3)$; my results for $SU(3)$ use my thermalization algorithm. It is also reasonably straightforward to apply it to $SU(2)$ Higgs theory; but here it must be remembered that the constraint is a

linear combination both of E fields and of π fields (the conjugate momentum of the Higgs doublet); the dissipation algorithm used in the thermalization should change both fields in proportion to their contribution to the Gauss constraint (holding U and ϕ fixed throughout the enforcement of the constraint). However, when the $SU(2)$ Higgs system is allowed to evolve according to the Hamiltonian equations of motion with a chemical potential for N_{CS} , the Gauss constraint should be enforced by only changing the E fields, since the spurious dynamics which arise when a term $\propto B$ is added to \dot{E} only add inappropriate terms to the E field; in other words the Higgs boson does not enter Eq. (34,36) except as an offset of C_\perp^α .

When applying the algorithm to the distorted lattice, it must be remembered to define orthogonality in terms of the quadratic part of the Hamiltonian. In other words, since Energy= $l(E_1^2 + E_2^2 + (l^{-1}E_3)^2)$, when we find the violation of the Gauss constraint $C_x = E_1 + E_2 + l^{-1}(l^{-1}E_3) - (\text{incoming lines})$, we should apply a correction of $-C_x$ to E_1 , to E_2 , and of $l^{-1}C_x$ to $l^{-1}E_3$; so although $l^{-2}E_3$ enters the Gauss constraint, E_3 is modified by C_x , with no power of l . The same dissipation algorithm should be used during the evolution of the fields with chemical potential as in the dissipative part of the thermalization, because the inner product defined by the dot product is the same as that defined by the Hamiltonian. It is never necessary to dissipatively enforce the Gauss constraint during the evolution step of the thermalization algorithm, because no chemical potential is applied and the equations of motion preserve the constraint identically, as I have of course verified numerically, for cubic and distorted lattices and for $SU(2)$ and $SU(3)$.

As a check that the algorithm correctly chooses E fields for the elongated lattice system, I thermalized the system with $l = 1.5$, ending by randomizing the E fields. I then allowed the system to evolve under the Hamiltonian equations of motion discussed in section 5, and checked to see if the distribution of energy between E_1 , E_2 and E_3 changed; it did not, to within statistical errors of less than 1%, showing that the thermalization correctly partitioned energy between these fields. (If I shift E_3 by $-l^{-2}C_x$ in the dissipation algorithm, which would be appropriate if I used the obvious rather than the correct metric on the E fields, then the energy distribution does shift.) The relation between Wilson loops in the normal and elongated directions also was not affected by randomizing the E fields and allowing the system to evolve.

I should comment that the thermalization problem cannot be solved by the following, very simple (but wrong), algorithm. Since the plaquette part of the Hamiltonian does not depend on the E fields, and the E field part is quadratic but with constraints, one uses a conventional lattice gauge theory algorithm to thermalize the plaquette part and then the above, simple algorithm to thermalize the E fields. The problem is that the constraints depend on the U fields; if we integrate over the (Gaussian) E fields we get a residual which is U field dependent and shifts the relative weights of different U field configurations; in fact it is exactly the A_0 fields of the dimensionally reduced theory. What we could do is use a standard lattice thermalization algorithm to thermalize the 3 dimensional system with plaquette action and A_0 fields with zero (bare) mass, use the resulting U fields, throw away the A_0 fields, and choose the E fields as discussed above.

Also, if we desired a new thermalization algorithm for the 3 dimensional plaquette action, without A_0 fields, we could do the following. Write down the Hamiltonian system but without Gauss constraints. Then the integral over E fields really is Gaussian with a total weight independent of the U field configuration, so thermalizing the system will produce the

correct population distribution for the U fields alone. We could then use the thermalization algorithm described above to generate U field configurations for the 3 dimensional Euclidean theory. Note that it is now completely trivial to choose the E field configuration. The algorithm completely randomizes the U fields with a number of computations which grows as 1 power higher than the number of space dimensions, which may make it an efficient algorithm for Euclidean lattice gauge theory on large lattices. It is also trivial to extend it to 4 Euclidean dimensions and to more complicated lattice actions.

References

- [1] G. t'Hooft, Phys. Rev. **D14**, 3432 (1976)
- [2] F. Klinkhammer and N. Manton, Phys. Rev. **D 30**, 2212 (1984)
- [3] P. Arnold and L. McLerran, Phys. Rev. **D 36**, 581 (1987)
- [4] V. Kuzmin, V. Rubakov, and M. Shaposhnikov, Phys. Lett. **155B**, 36 (1985)
- [5] A. Nelson, D. Kaplan, and A. Cohen, Nucl. Phys. **B 373**, 453 (1992)
- [6] M. Joyce, T. Prokopec, and N. Turok, Phys. Rev. **D 53**, 2930 (1996); Phys. Rev. **D 53**, 2958 (1996)
- [7] D. Grigorev and V. Rubakov, Nucl. Phys. **B 299**, 248 (1988)
- [8] J. Ambjorn, T. Askgaard, H. Porter, and M. Shaposhnikov, Nucl. Phys. **B 353**, 346 (1991)
- [9] J. Ambjorn and A. Krasnitz, Phys. Lett. **B 362**, 97 (1995)
- [10] A. Krasnitz, Nucl. Phys. **B 455**, 320 (1995)
- [11] A. Krasnitz, private communication
- [12] O. Philipsen, Phys. Lett. **B 358**, 210 (1995)
- [13] V. Rubakov and M. Shaposhnikov, hep-ph/9603208
- [14] R. Kubo, J. Phys. Soc. Jap. **12**, 570 (1957)
- [15] J. Kogut and L. Susskind, Phys. Rev. **D 11**, 395 (1975)
- [16] For a detailed account of dimensional reduction and its accuracy, see K. Farakos, K. Kajantie, K. Rummukainen, and M. Shaposhnikov, Nucl. Phys. **B 425**, 67 (1994), Phys. Lett. **B 336**, 494 (1994), Nucl. Phys. **B 442**, 317 (1995); K. Kajantie, M. Laine, K. Rummukainen, and M. Shaposhnikov, Nucl. Phys. **B 458**, 90 (1996), hep-lat/9510020
- [17] K. Kajantie, M. Laine, K. Rummukainen, and M. Shaposhnikov, Nucl. Phys. **B 458**, 90 (1996).

- [18] Neil Turok, private communication
- [19] D. Bodeker, L. McLerran, and A. Smilga, Phys. Rev. **D 52**, 4675 (1995)
- [20] E. Braaten and R. Pisarski, Phys. Rev. **D 42**, 2156 (1990)
- [21] L. McLerran, E. Mottola, and M. Shaposhnikov, Phys. Rev. **D 43**, 2027 (1991)
- [22] G. Giudice and M. Shaposhnikov, Phys. Lett. **B 326**, 118 (1994)
- [23] M. Dine and S. Thomas, Phys. Lett. **B 328**, 73 (1994)
- [24] N. Turok and J. Zadrozny, Phys. Rev. Lett. **65**, 2331 (1990), Nucl. Phys. **B 358**, 471 (1991); L. McLerran, M. Shaposhnikov, N. Turok, and M. Voloshin, Phys. Lett. **B 256**, 451 (1991)

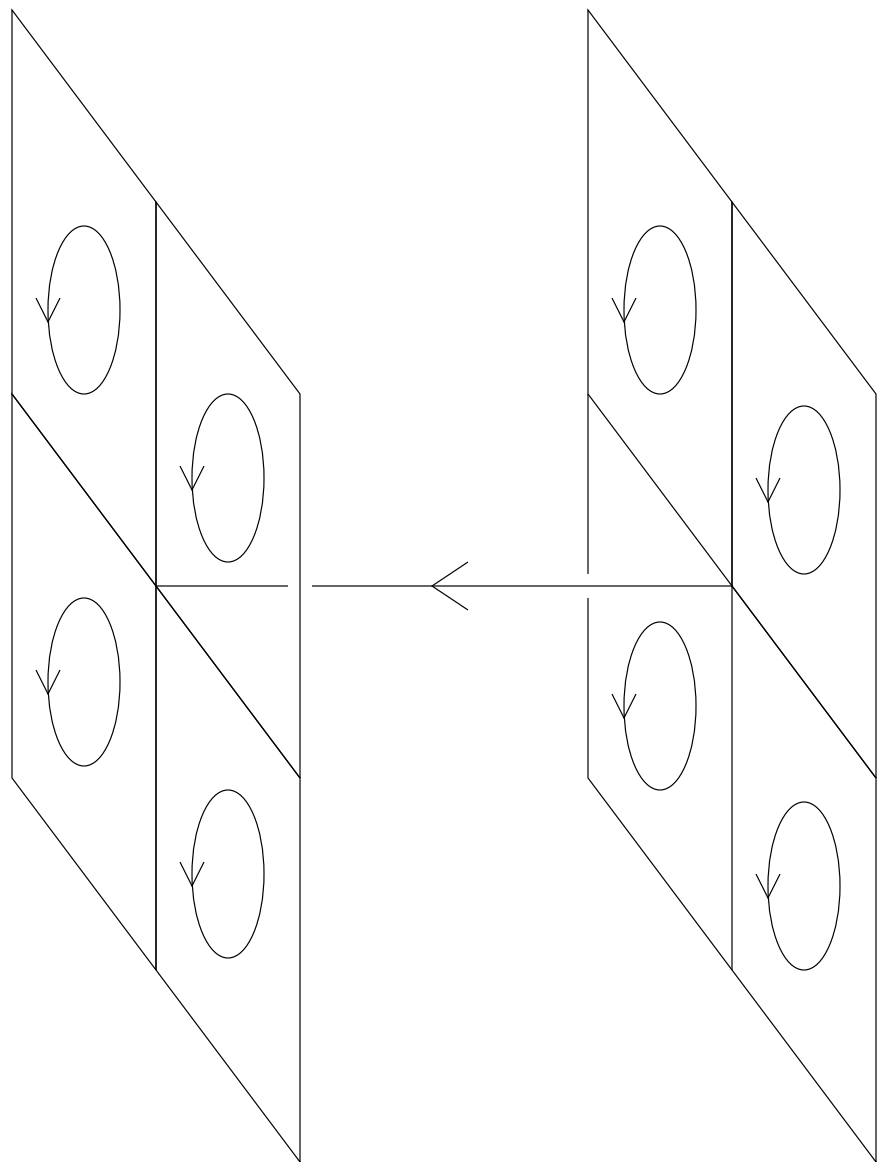
Figure 1: The 8 plaquettes contribute to the magnetic field along the vertical link.

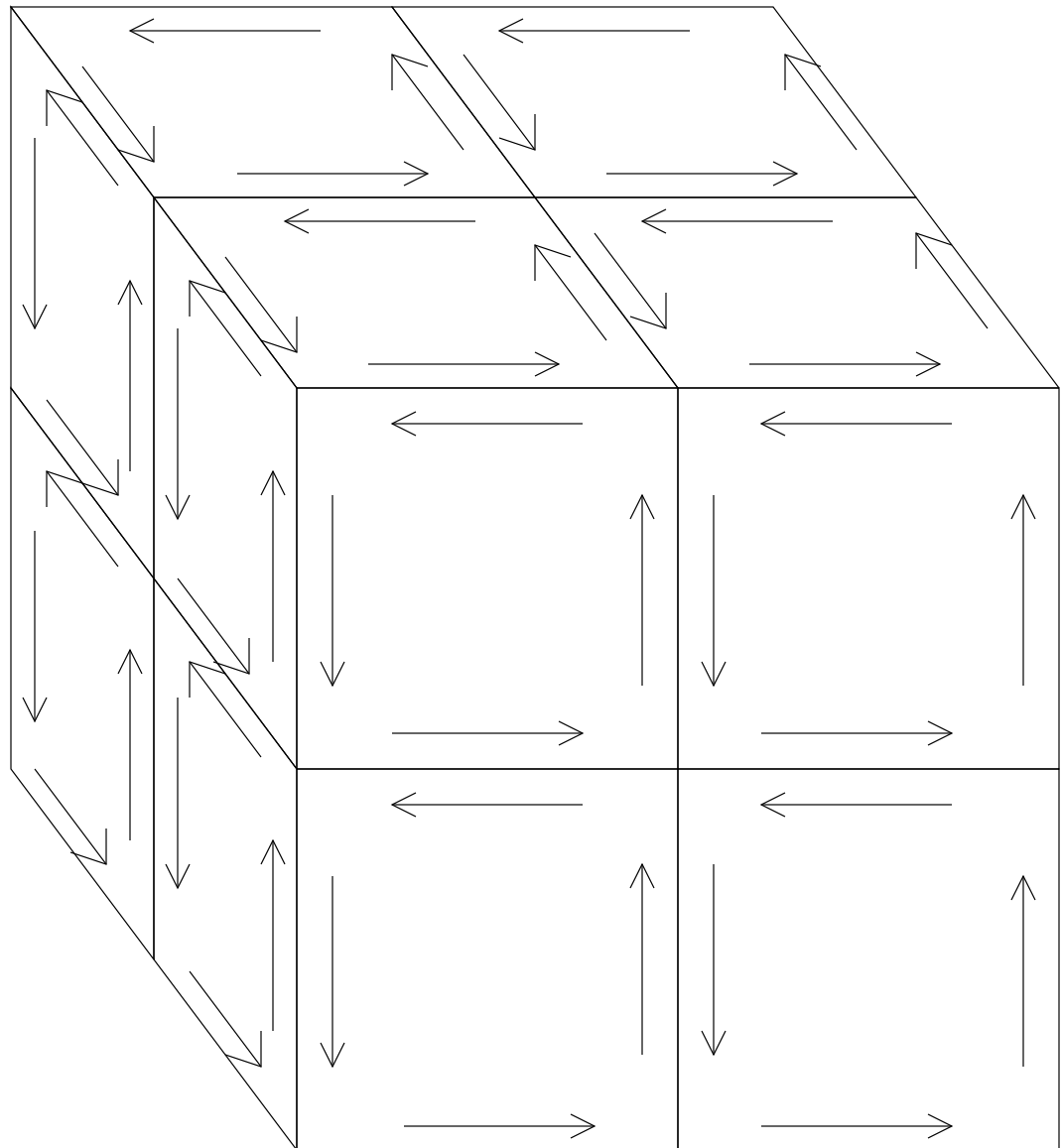
Figure 2: The configuration of non-identity links which will make the discrete spacetime integral of $F\tilde{F}$ nonzero; $U1 = 1 + i\epsilon\tau_1$, $U2 = 1 + i\epsilon\tau_2$, and $U3 = 1 + i\epsilon\tau_3$. Going around the plaquette containing $U1$ and $U2$ picks up an $O(\epsilon^2)$ contribution in the τ_3 Lie algebra direction, which gives a nonzero contribution when traced against the plaquette which goes backwards in time, even though all links at large distances are the identity.

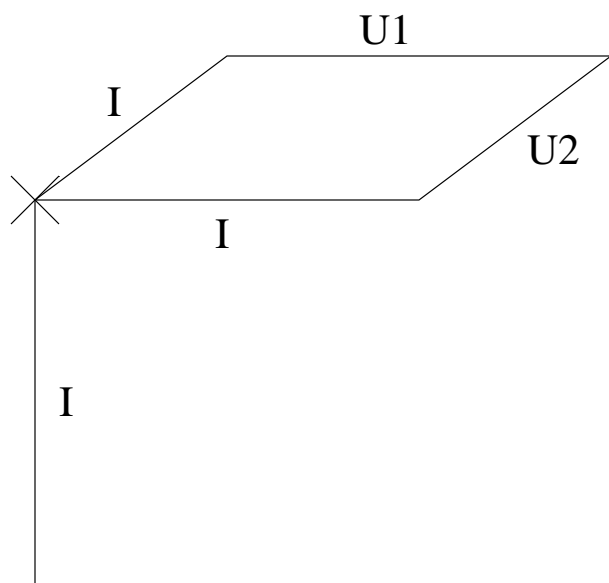
Figure 3: Contributions to $D_i E_i$ at a lattice point arise from the surface of the smallest box enclosing that point. Each link on the surface is traversed once with each orientation; in the abelian theory their contributions cancel, but in $SU(2)$ theory nonzero commutators arise.

Figure 4: Lattice size dependence of the rate \dot{N}_{CS} . The horizontal scale is N/β_L , the vertical scale is $\kappa(\mu\beta_L)$. If the rate arose out of ultraviolet physics then the curve would be flat.

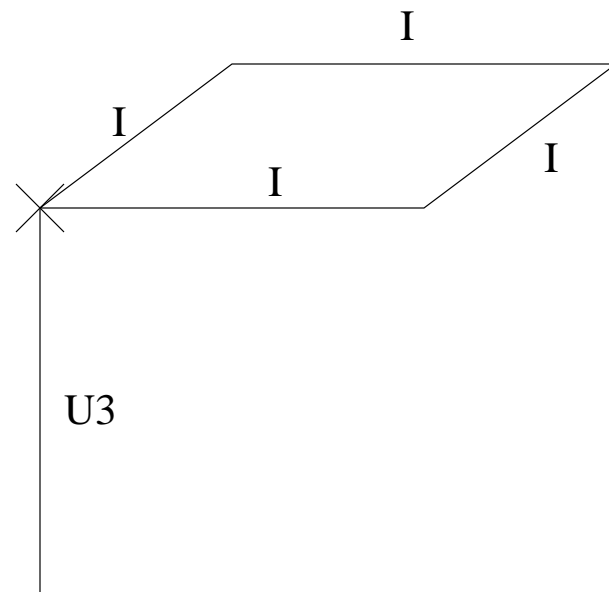
Figure 5: Dependence of \dot{N}_{CS} on μ . Horizontal scale is $\mu\beta_L$, vertical scale is $\dot{N}_{CS}(\pi\beta_L)^4/N^3$. The line is a reasonable best fit to the points at lower μ . The dependence is startlingly linear up to $\mu \sim 6/\beta_L$, demonstrating that there is not a free energy barrier to change in N_{CS} .







Link values at one time step



Link values at previous timestep

